Pharm Res (2012) 29:3373–3383
DOI 10.1007/s11095-012-0832-3

RESEARCH PAPER

# Preclinical Studies of YK-4-272, an Inhibitor of Class II Histone Deacetylases by Disruption of Nucleocytoplasmic Shuttling

Hye-Sik Kong • Shuo Tian • Yali Kong • Guanhua Du • Li Zhang • Mira Jung • Anatoly Dritschilo • Milton L. Brown

Received: 21 March 2012 / Accepted: 9 July 2012 / Published online: 27 July 2012


## ABSTRACT

***Purpose*** The HDAC shuttling inhibitor, YK-4-272 functions by restricting nuclear shuttling of Class II HDACs. Pre-clinical investigations of YK-4-272 bioavailability, pharmacokinetics, *in vivo* toxicity and tumor growth inhibition were performed to determine its potential as an HDAC shuttling disruptor for use in clinical applications.

***Methods*** The solubility, lipophilicity, *in vitro* metabolic stability, *in vitro* intestinal permeability, and *in vivo* pharmacokinetics of YK-4-272 were determined by HPLC methods. The anti-tumor activity of YK-4-272 was determined by monitoring athymic Balb/c nude mice bearing PC-3 xenografts.

***Results*** Oral bioavailability of YK-4-272 is supported by its solubility (0.537 mg/mL) and apparent partition coefficient of 2.0. The compound was chemically and metabolically stable and not a substrate for CYP450. In Caco-2 cell transport studies, YK-4-272 was highly permeable. The time-concentration profile of YK-4-272 in plasma resulted in a $C_{max}$ of 2.47 $\mu$g/mL at 0.25 h with a AUC of 3.304 $\mu g \times h$/mL. Treatment of PC-3 tumor xenografts with YK-4-272 showed significant growth delay.

***Conclusions*** YK-4-272 is stable and bio-available following oral administration. Growth inhibition of cancer cells and tumors was observed. These studies support advancing YK-4-272 for further evaluation as a novel HDAC shuttling inhibitor for use in cancer treatment.

Hye-Sik Kong and Shuo Tian contributed equally to this publication.

**Electronic supplementary material** The online version of this article (doi:10.1007/s11095-012-0832-3) contains supplementary material, which is available to authorized users.

**KEY WORDS** histone deacetylase shuttling disruptor · metabolism · YK-4-272

## ABBREVIATIONS

| | |
|---|---|
| AMMC | 3-[2-(N,N-diehtyl-N-methylamino)ethyl]-7-methoxy-4-methylcoumarin |
| BQ | 7-benzoyloxyquinoline |
| CEC | 3-cyano-7-ethoxycoumarin |
| CYP450 | Cytochrome P450 |
| MFC | 7-methoxy-4-triflouromethylcoumarin |
| MRP | multidrug resistance-associated protein |
| P-gp | P-glycoprotein |
| TEER | transepithelial electrical resistance |

## INTRODUCTION

Four classes of human histone deacetylases (HDACs) are based on structure, sequence homology, and domain organization. Class I enzymes play roles in cell proliferation and apoptosis and include nuclear HDACs 1, 2, 3, and 8 (1). Class IIA includes HDACs 4, 5, 7, and 9, class IIB includes HDACs 6 and 10, and may localize in the cytoplasm or translocate to the nucleus (2). These enzymes are characterized by a large

H.-S. Kong • Y. Kong • L. Zhang • M. Jung • A. Dritschilo • M. L. Brown
Department of Oncology, Lombardi Comprehensive Cancer Center
Georgetown University Medical Center
3970 Reservoir Road
Washington, District of Colombia 20057, USA

H.-S. Kong • Y. Kong • L. Zhang • M. L. Brown (✉)
Drug Discovery Program
Georgetown University Medical Center
3970 Reservoir Road
Washington, District of Colombia 20057, USA
e-mail: mb544@georgetown.edu

M. Jung • A. Dritschilo
Department of Radiation Medicine, Lombardi Comprehensive Cancer Center Georgetown University Medical Center
3970 Reservoir Road
Washington, District of Colombia 20057, USA

S. Tian • G. Du
Institute of Materia Medica
Chinese Academy of Medical Sciences & Peking Union Medical College
1 Xian Nong Tan Street
Beijing 100050, China

$NH_2$-terminal domain or a second catalytic site and their expression pattern in certain tissues are more restricted, suggesting roles in cellular differentiation and development (1). Class III enzymes, include the SIRTs (sirtuins), and are NAD-dependent deacetylases (3,4), and HDAC 11 has been placed in the new Class IV (5).

HDACs are involved in critical cellular functions, such as cell cycle regulation and apoptosis, although key functions of HDACs lie in their capacity for transcriptional regulation. By functioning as components of large multi-protein complexes, HDACs bind to promoters and repress transcription. Reported acetylation mechanisms have involved histones and various non-histone proteins, including tubulin (6–9).

Class II compounds shuttle between the cytoplasm and the nucleus; however, both classes of HDACs have conserved deacetylase core domains of approximately 400 amino acids and zinc binding sites (3). The core domain has represented the principal target for design of inhibitory small molecules, however restriction of Class II HDAC shuttling from the cytoplasm to the nucleus may also serve as a mechanism for functional inhibition. For example, the recruitment of the Class II HDAC4 to the nuclei of hormone resistant prostate cancer cells exerts an inhibitory effect on differentiation and contributes to the development of an aggressive phenotype of late stage prostate cancer (10).

We have reported the discovery of a novel hydroxamic HDAC inhibitor (YK-4-272) with intrinsic fluorescent properties and have noted restriction of the molecule to the cytoplasmic sub-cellular compartment (11). YK-4-272, also called compound 2, is a disruptor of HDAC shuttling (11). Also, we have advanced the hypothesis that cytoplasmic restriction of Class II HDACS contributes to inhibitor target selectivity and novelty. Here, we report preclinical studies in support of YK-4-272 as a candidate HDAC shuttling inhibitor suitable for clinical translation.

## MATERIALS AND METHODS

### Chemicals

Propranolol, atenolol, verapamil, MK-571, D-Glucose 6-phosphate sodium salt, Glucose-6-phosphate dehydrogenase (G-6-PDH), β-Nicotinamide adenine dinucleotide phosphate sodium salt ($NADP^+$), Dimethyl Sulphoxide (DMSO), non-essential amino acids (NEAA), Hydrogen peroxide, 1-Octanol, Magnesium chloride, Tween80, Acetic acid, Phosphoric acid, Sodium phosphate monobasic monohydrate, and Sodium phosphate dibasic were purchased from Sigma (St. Louis, MO). Fetal bovine serum (FBS), Hepes, Glutamine, and Penicillin/streptomycin were from Invitrogen (Grand Island, NY). Hank's Balanced Salt Solution (HBSS), Phosphate-Buffered Saline (PBS), and Sodium pyruvate were from Cellgro (Manassas, VA). Polyethylene glycol 400 (PEG) was from Hampton (Aliso Viejo, CA). Hydrochloric acid, Xylene, Tween20, Paraffin phosphate buffer, Formalin, HPLC grade-acetonitrile, ethanol, ethyl acetate, and methanol were from Fisher Scientific Co (Pittsburgh, PA).

### Animals

Pharmacokinetic studies of YK-4-272 were evaluated in male Sprague-Dawley rat with a weight of 225 ± 10 g. The animal was fasted for 12 h and had free access to water prior to the experiment. Female and male Balb/c mice and athymic Balb/c nude mice were purchased from the National Cancer Institute (NCI). Female Balb/c mice were used for the toxicity study, male Balb/c and athymic Balb/c nude mice were used for xenograft study of YK-4-272. Animals were housed 4–6 per cage with microisolater tops. Food (Furina mice chow) and water were provided *ad libitum*. Female mice are nulliparous and non-pregnant. The light cycle was regulated automatically (12 h light/dark cycle) and the temperature was maintained at 23 ± 1°C. All animals were allowed to acclimate to this environment for one week prior to experimental manipulations. The protocol involving animal use is approved by the Georgetown University Animal Welfare Committee (#11-029) and conducted pursuant to the Animal Care guidelines.

### Preparation of YK-4-272

For this study, we prepared YK-4-272, also called compound 2, as described in the reported supplemental method (11).

### Solubility and pH Chemical Stability

To determine solubility, 20 mg of YK-4-272 was shaken in 1 mL of an isotonic phosphate buffer solution (pH 6.8) at 25°C for 24 h. After centrifugation, the concentration of YK-4-272 in a 50 μL portion of the supernatant was analyzed by HPLC. To determine chemical stability, a 1 mM solution of YK-4-272 was incubated in pH 1.2 hydrochloric acid buffer or pH 6.8 isotonic phosphate buffer at 37°C for 24 h. At pre-determined intervals, 500 μL aliquots were removed, and the concentrations of YK-4-272 were determined by HPLC.

### Apparent Partition Coefficient

The apparent partition coefficient of YK-4-272 was determined as previously reported (12,13). Briefly, 10 mL of YK-4-272 solution (1 mM) in pH 6.8 isotonic phosphate buffer pre-saturated with 1-octanol was added to 10 mL of 1-

octanol pre-saturated with pH 6.8 isotonic phosphate buffer. The mixture was shaken for 10 h and allowed to stand for 6 h at 37°C. The concentration of YK-4-272 in the aqueous phase was analyzed by HPLC. The apparent partition coefficient was calculated by employing the following equation. $P = (C_o - C_w)/C_w$, where $C_o$ and $C_w$ represent the initial and equilibrium concentration of the compound in aqueous phase, respectively. $C_o - C_w$ is the concentration of the compound partitioned in the octanol layer.

### Cell Culture

Caco-2 cells were obtained from the Tissue Culture Shared Resources of the Lombardi Comprehensive Cancer Center in Georgetown University Medical Center (Washington, DC) and cultured in Dulbecco's modified Eagle medium (DMEM, Cellgro, Manassas, VA). The medium was supplemented with 10% fetal bovine serum (FBS), non-essential amino acids (NEAA), glutamine, Hepes, sodium pyruvate, and penicillin/streptomycin. For the transport studies, a 24-well BIOCOAT® HTS Fibrillar Collagen Multiwell™ Insert System was purchased from BD Biosciences (Bedford, MA) and Caco-2 cells were seeded at a density of $6\times10^5$ cells/cm$^2$ on 24-well and cultured in the seeding medium by following the manufacturer's instructions (14). After culturing for 24 h, the medium was replaced with the cell differentiation-inducing medium and incubated for 72 h. For xenograft study, PC-3 cells (ATCC, Manassas, VA) were cultured in DMEM with L-glutamine (Mediatech Inc., Herdon, VA) containing 5% fetal bovine serum (FBS), 2.5 mM L-glutamine at 37°C with 5% $CO_2$.

### Transport Studies

Caco-2 cells were monolayered in a 24-well plate format. The trans-epithelial electrical resistance (TEER), a value of the integrity of each chamber containing Caco-2 cell monolayer was measured using a Millicell-ERS Voltohmmeter (Millipore Corp., Bedford, MA). The TEER values were measured before and after transport studies and only values greater than 400Ω/cm$^2$ were used for the transport assay. The integrity of the monolayer was also determined by Lucifer yellow passage (%) across the monolayer for 1 h using fluorescence, excitation wavelengths of 485 nm and emission of 535 nm. The Caco-2 cell monolayers were pre-incubated with pre-warmed HBSS buffer (pH 7.4) at 37°C and 5% $CO_2$ for 10 min. 100 μM concentrations of the test compound in pre-warmed HBSS buffer were added to either the apical or basolateral side of the monolayer. The volumes on the apical and basolateral chambers were 0.5 and 1.0 mL, respectively. The donor compartment concentration (100 μM) was determined by HPLC before and after incubation for the recovery and the flux calculation. The test plate was incubated and shaken at 37°C, 5% $CO_2$, 100% humidity, and 50 rpm for 2 h. At indicated intervals, aliquots of 500 μL were taken from each receiver chamber and replaced with equal volumes of HBSS buffer. The concentrations of test compound were determined by HPLC. The efflux ratio values were calculated by employing $P_{app}$B-A/$P_{app}$A-B. As a standard compound, propranolol and atenolol were evaluated for high permeability exhibition and low permeability exhibition, respectively (15,16).

### Metabolic Stability

*InVitro* CYP™ H-class 10-donor mixed gender pooled human liver microsomes were obtained from Celsis *In Vitro* Technologies Inc. (Baltimore, MD). The reaction mixture consisted of human liver microsomes (1 mg/mL), G-6-PDH (2U/mL), glucose 6-phosphate (10 mM), and $NADP^+$ (1 mM) in 100 mM of PBS (pH 7.4) containing 10 mM of $MgCl_2$ was prepared (17,18). The mixture was pre-incubated and shaken at 37°C, 5% $CO_2$, 100% humidity, and 50 rpm for 10 min. 10 μM of YK-4-272 was added to the mixture, incubated and shaken at 37°C, 100% humidity, and 50 rpm for 2 h. At the pre-determined intervals, 200 μL aliquots were added to 800 μL of ice-cold stop solution consisting of acetonitrile/methanol (50/50, v/v). The concentrations of YK-4-272 were determined by HPLC.

### Cytochrome P450 Inhibition

Human recombinant CYP450-selective enzymes, CYP1A2/CEC, CYP2C9/MFC, CYP2C19/CEC, CYP2D6/AMMC, and CYP3A4/BQ high throughput inhibition screening kits, were purchased from BD Biosciences (Bedford, MA). The CYP450 inhibition assays were performed by following the manufacturer's instructions. 10 mM of YK-4-272 (50 μL) or of positive controls (50 μL) of selective enzymes were prepared in acetonitrile in 96-well black microtiter plates and pre-incubated with NADPH-regenerating system (100 μL) at 37°C for 10 min. The reaction was initiated by the addition of enzyme/substrate mixture (100 μL) and incubated at 37°C for 15, 30, or 45 min. Cold stop reagents (75 μL) composed of acetonitrile/0.5 M Tris base (80/20, v/v) were added. The concentration of YK-4-272 or positive control was analyzed by fluorescence measurement.

### Time-Concentration Profiles of YK-4-272 in Plasma After Oral Administration to Rats

Five male Sprague-Dawley rats weighing 225±10 g fasted for 12 h with free access to water prior to the experiment. 100 mg/kg of YK-4-272 suspension was prepared with

0.5% Tween 80 aqueous solution. Blood samples were collected pre-dose and subsequently at 0.083, 0.25, 0.5, 0.75, 1, 1.5, 2, 2.5, 3, 4 and 5 h after oral administration of YK-4-272. The blood samples were centrifuged at 5,000 rpm for 10 min at 4°C. The centrifuge is Allegra™ X-22R (Beckman Coulter, USA) equipment with the rotor of F2402 in this experiment. 100 μL of plasma was transferred and stored at −20°C until analysis. A 100 μL volume of blank plasma, calibration standards or plasma samples were spiked into 1 mL of ethyl acetate. After a 3 min vortex and 10 min centrifugation at 13,400 rpm at 4°C, the organic layer was evaporated under $N_2$ to dryness and reconstituted with 100 μL volume of methanol. The sample was transferred immediately to 1.5 mL auto sampler vial and 20 μL were used for HPLC analyses. For the analysis method development and validation, accuracy, precision, recovery, and stability of YK-4-272 in plasma after oral administration was measured, please see Supplementary Material Table I.

## HPLC Analytical Method

The HPLC system consists of a CBM-20A connector, a DGU-20A degasser, LC-20 AD pumps, a SDP-10AV UV detector, and a SIL-$HT_A$ Shimadzu autosampler. A Waters Symmetry® C18 column (4.6×250 mm, 5 μm) equipped with a C18 guard column was used. The mobile phase was eluted through the column at a flow rate of 1.0 mL/min. The mobile phase for YK-4-272 consisted of 25% acetonitrile in water containing 0.05% phosphoric acid. For propranolol, the mobile phase consisted of 20% acetonitrile in water containing 0.1% acetic acid. For atenolol, the mobile phase consisted of 25% acetonitrile in water containing 0.1% triethylamine. The eluent was monitored at 220 nm for YK-4-272 and 254 nm for propranolol and atenolol by the UV detector measuring the absorption with a sensitivity of AUFS 0.01. The retention time of YK-4-272, propranolol, and atenolol was 9.68, 6.92, and 5.10 min, respectively. Standard curves were linear in the range of 0.01–1000 μg/mL of stock solutions of compounds ($r^2$=0.999). And for SD rat pharmacokinetic studies of YK-4-272, we used Agilent HPLC 1200 system. Agilent Zorbax SB-C18 column (4.6× 150 mm, 5 μm) equipped with an Agilent Zorbax SB-C18 guard column (4.6×12.5 mm, 5 μm) was used and column temperature was at 40°C. The mobile phase of this system consisted of 23% acetonitrile in water containing 0.05% phosphoric acid for YK-4-272 and eluted at a flow rate of 1.0 mL/min. The UV absorption was at wavelength 222 nm.

## Acute Toxicity Study

By following the protocol for Acute Toxicity-Up-and Down Procedure (19), YK4-272 was administered in a constant volume (0.01 mL/1 g body weight) over the range of doses. The stock solution was prepared using DMSO and PEG at 1:1 ratio, and the concentration was 200 mg/mL. The working solution was diluted in polyethylene glycol (PEG). Animals were dosed by intra-peritoneal (i.p.) injection and uninterrupted observation was maintained for the first 4 h. Sequencial daily observations were performed for 14 days. Animals were sacrificed and necropsy was performed. All pathological findings were recorded. The organs from the death animals were stored in 10% formalin solution for further histopathological examination. The $LD_{50}$ and confidence interval of YK-4-272 were determined by AOT 425 StatPgm.

## Xenograft Study

Evaluation of effects of YK-4-272 on mouse xenograft was performed as previously reported (20). Briefly, male athymic Balb/c nude mice weighing 18–22 g were injected with 0.3 mL of $3\times10^6$ PC-3 cells in the subcutaneous tissue of the right axillary region of the body. One week after the injection, the mice were randomly sorted into two groups of four mice each. A 1 g/mL stock solution of YK-4-272 in DMSO was prepared and PEG 400 (Hampton) and PBS with a 1:1 ratio was added to make the test concentration. The tumor-bearing mice received an i.p. with either 10 mg/kg of YK-4-272 or vehicle control once every other day for 5 weeks. At the same time, the tumor size of each mouse was measured by caliper and calculated by the formula: Length×width×height/2.

## Immunohistochemical Staining Detection of HDAC4 Protein

Nude mice bearing PC3 xenografted tumors were treated with YK-4-272 for 30 days and euthanized. Tumors were separated and then fixed with 10% paraffin phosphate buffer. De-paraffinized and re-hydrated as follow: 2× 10 min soaked in Xylene followed by 3 min in a graded series of ethanol to distilled water. Tumor sections were boiled in citrate buffer (10 mM Citrate, plus 0.05% Tween20, pH 6.0) for 20 min to induce epitope retrieval, and the slides were allowed to cool for 20 min at room temperature, followed by a distilled water rinse. Slides were incubated with 3% hydrogen peroxide to block endogenous peroxidase activation for 10 min at room temperature. Slides were rinsed in 1X Tris buffered saline with 0.05% Tween20 (TBS-T) for 5 min, and incubated with 10% normal goat serum for 10 min at room temperature. The serum was decanted and incubated with rabbit anti-HDAC4 antibody (Abcam, ab1437), diluted in 1X TBS-T with 5% NGS at 1:1000 dilution for 1 h at room temperature. A biotin conjugated anti-Rabbit (Vector Labs, BA-1000) secondary antibody was applied at a 1:200 dilution

for 30 min at room temperature and then incubated with ABC reagent (Vector Labs, PK-6100) for 30 min at room temperature. Tumor sections were incubated with DAB chromagen (Dako, K3469). The tumors receiving no treatment were incubated with primary antibody.

### Detection of HDAC4 Expression in Xenograft Tumor Treated with YK-4-272 for 30 days

The expression levels of HDAC4 in PC3 xenografts tumors treated with YK-4-272 for 30 days were analyzed by Western blotting. Briefly, tumors were sonicated for 20 s with 50% pulse in cold RIPA (Pierce, 89900) with protease inhibitor cocktail (Pierce, 78410) and Halt phosphatase inhibitor cocktail (Pierce, 78420). The tumors were kept on ice for 20 min with manual swirling in a microcentrifuge tube, and the mixture was centrifuged at 14,000×g for 20 min to pellet the tissue debris. Protein containing supernatant was collected and the protein concentration in the supernatant was measured. Samples (25 µg) were separated on 4%–20% Tris-Glycine SDS/PAGE (Invitrogen NP0316) and transferred to PVDF (Invitrogen, LC2005) membranes for immunoblotting with HDAC4 antibody (Abcam, ab1437). Actin antibody (Santacruz, sc-1615) was used for loading control.

### Data Analysis

Apparent permeability coefficients ($P_{app}$, cm/sec) were calculated by employing the following equation (21,22):

$$\text{Papp} = \frac{V}{A \times Co} \times \frac{dQ}{dt}$$

where V is the volume (mL) in acceptor compartment, A is the membrane surface area ($cm^2$), and $C_0$ is the initial concentration of test compound in the donor compartment (nmol/mL). dQ/dt is the appearance rate of the test compound at the receiver side (nmol/mL s). For the CYP450 inhibition studies, high concentrations and low concentrations of test compound bracket the 50% inhibition value were determined by plotting % activity *versus* concentration (23).

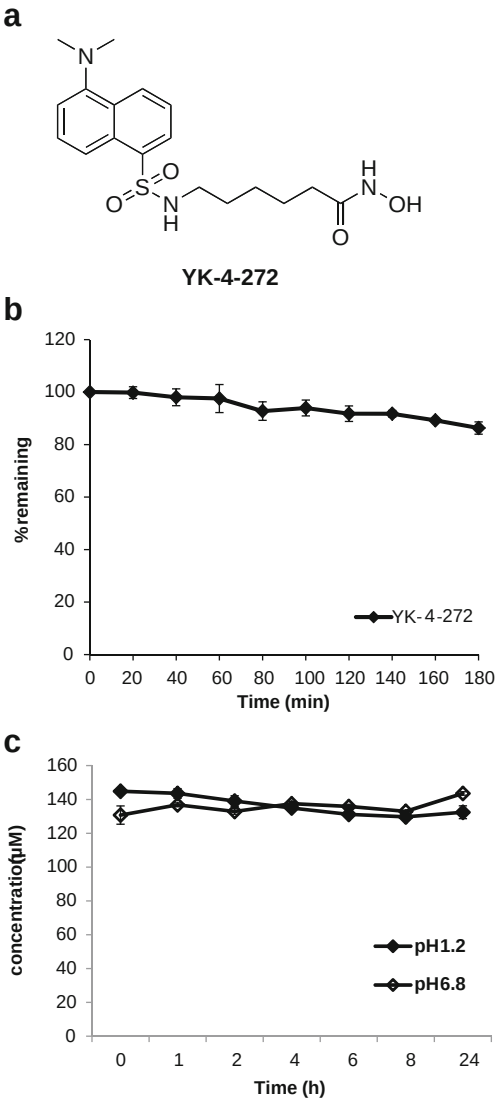


**Fig. 1** (**a**) Chemical structure of YK-4-272. (**b**) Metabolic stability of YK-4-272 in human liver microsomes. 10 µM of YK-4-272 was incubated with 10-donor mixed gender pooled human liver microsomes (1 mg/mL) for 2 h. (**c**) Chemical stability of YK-4-272. YK-4-272 was incubated in pH 1.2 hydrochloric acid buffer or pH 6.8 isotonic phosphate buffer at 37°C for 24 h. At the appropriate time intervals, depletion of YK-4-272 was monitored by analyzing the concentration of YK-4-272 through HPLC. Each bar represents the mean ± S.D. ($n$=3).

## RESULTS

### Solubility, pH Stability and Apparent Partition Coefficient

The chemical structure of YK-4-272 is shown in Fig. 1a. The solubility of YK-4-272 was 0.537 mg/mL in pH 6.8 isotonic phosphate buffer at 25°C. YK-4-272 was chemically stable in pH 1.2 or 6.8 buffer solution at 37°C for 24 h (Fig. 1c). The apparent partition coefficient of YK-4-272 in 1-octanol/phosphate-buffered (pH6.8) solution was 2.0 at 37°C.

### Transport Studies

The Caco-2 cell monolayer permeability test is a well-developed *in vitro* strategy for predicting gastrointestinal tract drug transport (17). Caco-2 efflux proteins contain P-glycoprotein (P-gp) and other members of the multidrug resistance-associated protein (MRP) family known to mediate trans-membrane drug transport (24). These proteins are associated with chemotherapy resistance mediated by increases in ATP-binding cassette (ABC) transport proteins which include P-gp and MRP (25). Therefore, intestinal transport of

**Table I** Permeability ($P_{app}$) and Efflux Ratio of YK-4-272 Across Caco-2 Cell Monolayers. Bidirectional Transport of YK-4-272 was Observed Across Caco-2 Cell Monolayers for 2 h. Highly Permeable Propranolol and Lowly Permeable Atenolol were Evaluated as Standard Compounds. Data Are Expressed as Mean ± S.D. ($n$=3)

| Compound (concentration) | Drug Transport $P_{app}$ ($\times 10^{-6}$ cm/sec) | | Efflux ratio |
|---|---|---|---|
| | A→B | B→A | |
| YK-4-272 (100 μM) | 20.7 ± 0.05 | 20.2 ± 0.05 | 0.98 |
| Propranolol (100 μM) | 41.6 ± 2.40 | 21.3 ± 0.70 | 0.51 |
| Atenolol (100 μM) | 3.1 ± 0.01 | 1.9 ± 0.01 | 0.61 |

Efflux ratio=$P_{app}$B-A/$P_{app}$A-B

anticancer drugs may be affected when P-gp or MRP substrate, inhibitors or inducers are co-administrated. Transport studies using human colonic adenocarcinoma Caco-2 cells can provide an early estimation of barriers to gastrointestinal tract absorption and cell membrane permeation of drug, therefore bioavailability of drug can be determined (26). The transport of 100 μM of YK-4-272 across Caco-2 cell monolayer was monitored for 2 h in both apical to basolateral and basolateral to apical directions. The permeation rates in both apical to basolateral and basolateral to apical direction were calculated from the slope of the concentration *vs.* time graph using linear regression. Table I summarizes the $P_{app}$ values for permeation of the compounds across Caco-2 cell monolayers in both directions. YK-4-272 exhibited $P_{app}$ values of $20.7\times10^{-6}$ cm/sec in the apical to basolateral direction and $20.2\times10^{-6}$ cm/sec in the basolateral to apical direction. To examine our Caco-2 transport system efficiency, the well-known low permeability marker, atenolol (16), and the high permeability marker, propranolol (15) were tested, showing that 100 μM of atenolol exhibited $P_{app}$ values of $3.1\times10^{-6}$ cm/sec in the apical to basolateral direction and $1.9\times10^{-6}$ cm/sec in the basolateral to apical direction, and 100 μM of propranolol exhibited $P_{app}$ values of $41.6\times10^{-6}$ cm/sec in apical to basolateral direction and $21.3\times10^{-6}$ cm/sec in basolateral to apical direction (Table I). Caco-2 cells express P-gp, MRP1, and MRP2 proteins which can mediate the efflux of a variety of drugs through the Caco-2 cell monolayers (24). Based on FDA guidance, the compound which has an efflux ratio greater than 2 can be a substrate or inhibitor of P-gp (17,27). The efflux ratio of YK-4-272 is about 1 (Table I). These data demonstrate that YK-4-272 might be transported well through the GI tract without limitation by P-gp or MRP1/MRP2.

## Metabolic Stability in Human Liver Microsomes

To examine the oral bioavailability of YK-4-272, *in vitro* metabolic stability of YK-4-272 was determined in 10-donor mixed gender pooled human liver microsomes. YK-4-272 at a concentration of 10 μM was stable in the presence of human liver microsomes with the cofactors by monitoring disappearance of the parent compound over the incubation period (Fig. 1b). YK-4-272 showed a decrease of 14% over the 2 h period and no new chemical entities were detected by HPLC. As a positive control of human liver microsomes activity, 10 μM of docetaxel, a taxoid, was also evaluated (28), showing that 45% of the parent compound was metabolized rapidly over the 2 h incubation period (data not shown).

## Cytochrome P450 Metabolism

Cytochrome P450s are mainly involved in metabolic depletion of drugs through oxidative metabolism (29). To examine the potential of YK-4-272 for CYP450-mediated metabolism,

**Table II** Summary of Assay Conditions for CYP450 Inhibition

| Enzyme | CYP1A2 | CYP2C9 | CYP2C19 | CYP2D6 | CYP3A4 |
|---|---|---|---|---|---|
| Enzyme/well (pmol) | 0.5 | 1 | 1 | 1.5 | 1.53 |
| Phosphate buffer pH 7.4 (mM) | 100 | 100 | 100 | 100 | 200 |
| Glucose-6-phosphate (mM) | 0.825 | 0.825 | 0.825 | 0.825 | 0.825 |
| NADP+(μM) | 16.25 | 16.25 | 16.25 | 16.25 | 16.25 |
| G-6-PDH (Units/mL) | 0.4 | 0.4 | 0.4 | 0.4 | 0.4 |
| Substrate | CEC | MFC | CEC | AMMC | BQ |
| Substrate conc. (μM) | 5 | 75 | 25 | 1.5 | 40 |
| Positive control | Furafylline | Sulfaphenazole | Tranylcypromine | Quinidine | Ketoconazole |
| Positive control conc. (μM) | 120 | 12 | 120 | 0.6 | 6 |
| Incubation time (min) | 15 | 45 | 30 | 30 | 30 |
| Excitation wavelength (nm) | 410 | 410 | 410 | 390 | 410 |
| Emission wavelength (nm) | 460 | 530 | 460 | 460 | 530 |

*CEC* 3-cyano-7-ethoxycoumarin; *MFC* 7-methoxy-4-triflouromethylcoumarin; *AMMC* 3-[2-(N,N-diehtyl-N-methylamino)ethyl]-7-methoxy-4-methylcoumarin; *BQ* 7-benzoyloxyquinoline

YK-4-272 was incubated with human recombinant CYP450-selective enzymes, CYP1A2, 2C9, 2C19, 2D6, and 3A4. As seen in Table II, each positive control and the composition of the assay were summarized. The dose-response curves were demonstrated for YK-4-272 and each positive compound in Fig. 2. YK-4-272 weakly inhibited the activity of CYP1A2 exhibited by an $IC_{50}$ (Fig. 2a and Table III). Interestingly, YK-4-272 did not show any competitive inhibition of CYP3A4, 2C9, 2C19, 2D6 activity (Fig. 2b). The reference compounds, furafylline, sulfaphenazole, tranylcypromine, quinidine, and ketoconazole demonstrated $IC_{50}$ values of 8.34, 0.58, 9.86, 0.013, and 0.124 μM, for CYP1A2, 2C9, 2C19, 2D6, and 3A4, respectively (Fig. 2c and Table III).

## Time-Concentration Profiles of YK-4-272 in Plasma After Oral Administration to Rats

The permeability data and proper partition coefficient suggest good systemic absorption of YK-4-272. To verify that the systemic absorption of YK-4-272 was good *in vivo*, YK-4-272 was administered to rats by a gastric intubation and the levels of YK-4-272 in the blood collected for 5 h were monitored. As shown in Fig. 3, the time-concentration profiles of YK-4-272 in plasma after oral administration to rats showed that the $C_{max}$ was 2.47 μg/mL at 0.25 h and the AUC was 3.304 μg×h/mL after YK-4-272 administration. We summarized the pharmacokinetic data of YK-4-272 in Table IV. The data suggest that YK-4-272 demonstrates sufficient *in vivo* absorption following oral administration.

Inhibition of CYP450-mediated metabolism can underlie a mechanism for toxicities from drug-drug interactions. Compounds have been withdrawn from clinical trials because they have been shown to inhibit the metabolism of co-administered drugs or to release toxic metabolites (26). The cytochrome P450s (CYP) superfamily are the principal enzymes for the oxidative metabolism of drugs and xenobiotics and play a major role in the phase-I metabolism of almost all the clinically used drugs (30). The inactivation of a particular CYP can lead to serious side effects of drugs, resulting in increased clearance or reduced intestinal absorption. The most commonly responsible CYP450 enzymes for the metabolism of drugs are CYP1A2, CYP2C9, CYP2C19, CYP2D6, and CYP3A4 (30). Early evaluation of candidate small molecules is desirable to examine the metabolic stability, metabolism by CYP450, and intestinal transport of profiling potential toxicity and assessing bioavailability. These evaluations provide important predictions on safety and efficacy properties of a drug or its active metabolites.

Nuclear acetylation of histones is central to regulation of gene expression through chromatin modification and is determined by histone acetyltranferases (HATs) and histone deacetylases (HDAC) (31). We have reported a new class of compounds that disrupt the shuttling of HDACs into the

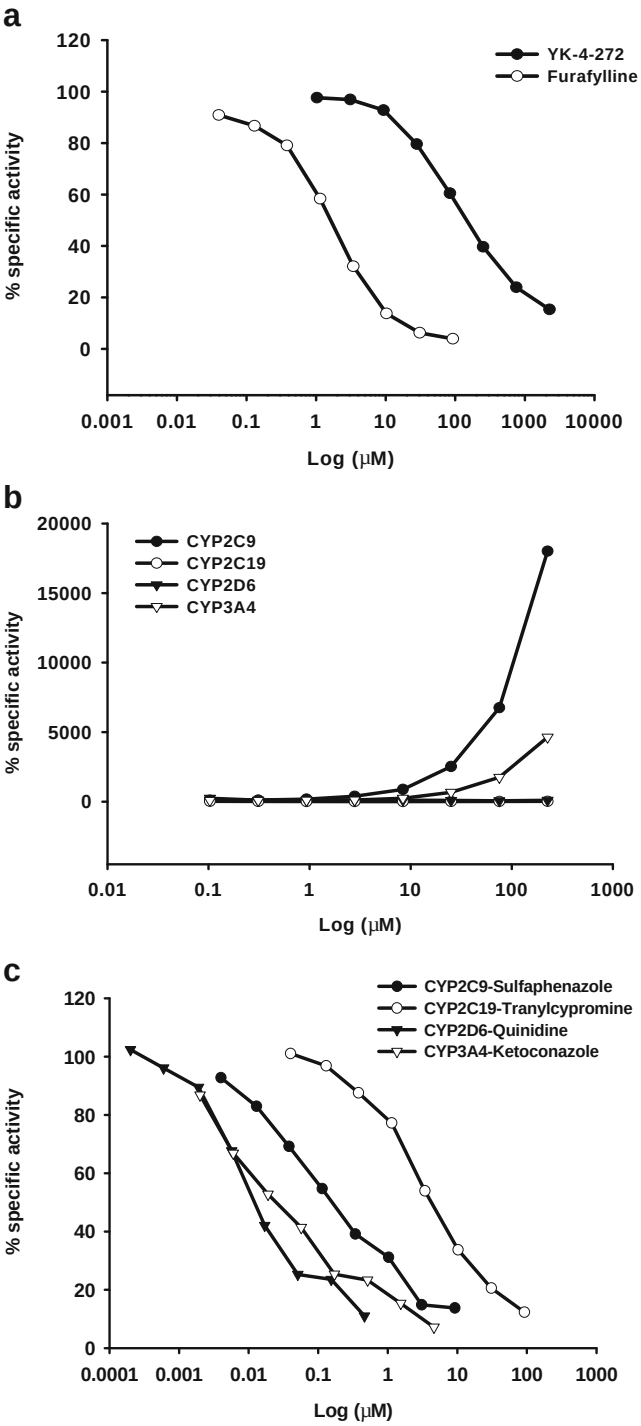


**Fig. 2** Cytochrome P450 metabolism of YK-4-272. Specific activity (%) of YK-4-272 and reference compounds (furafylline, sulfaphenazole, tranylcypromine, quinidine, and ketoconazole) on CYP1A2, 2 C9, 2 C19, 2D6, and 3A4 high throughput inhibition screening is shown in a dose range from 0.001 to 1000 μM (logarithmic scale). (**a**) % specific activity of YK-4-272 and furafylline on CYP1A2. (**b**) % specific activity of sulfaphenazole, tranylcypromine, quinidine, and ketoconazole on CYP2C9, 2 C19, 2D6, and 3A4, respectively. (**c**) % specific activity of YK-4-272 on CYP2C9, 2C19, 2D6, and 3A4. The mean of duplicate analysis is shown.

**Table III** $IC_{50}$ Values ($\mu$M) of YK-4-272 and Reference Compounds on CYP450 Activity. Data Are Expressed as Mean ± S.D. ($n$=3)

| Compound | Enzyme | | | | |
|---|---|---|---|---|---|
| | CYP1A2 | CYP2C9 | CYP2C19 | CYP2D6 | CYP3A4 |
| YK-4-272 | 166.80 ± 0.05 | NA | NA | NA | NA |
| Furafylline | 2.69 ± 0.003 | NT | NT | NT | NT |
| Sulfaphenazole | NT | 0.27 ± 0.003 | NT | NT | NT |
| Tranylcypromine | NT | NT | 8.92 ± 0.002 | NT | NT |
| Quinidine | NT | NT | NT | 0.01 ± 0.001 | NT |
| Ketoconazole | NT | NT | NT | NT | 0.05 ± 0.003 |

NA not available; NT not tested

nucleus (11). Furthermore, based on YK-4-272 intrinsic fluorescent properties, we have observed the cytoplasmic shuttling cellular localization of the drug. An expected outcome of HDAC inhibition/shuttling disruption YK-4-272 includes cancer growth inhibition. Therefore, we tested YK-4-272 oral administration and effects on human prostate (PC-3) tumor growth in mice.

### Antitumor Activity of YK-4-272 Using Xenograft Study

The acute toxicity of YK-4-272 was measured in female Balb/c mice by using the acute oral toxicity (AOT) up-and–down procedure (19). Estimated $LD_{50}$ was 550 mg/kg (the one dose with partial response). 95% profile likelihood confidence interval was 161.9 to 1750. To evaluate the antitumor activity of YK-4-272 *in vivo*, athymic Balb/c nude mice with human prostate tumor xenografts were treated *via* intraperitoneal injection with 10 mg/kg of YK-4-272 once a day every other day for 5 weeks. Control mice were injected with vehicle alone. As shown in Fig. 4a, 10 mg/kg dose of YK-4-272 effectively reduced tumor growth in mice by ~50% compared to control mice over 30 days. No body weight loss or mortality was detected in mice receiving vehicle or YK-4-272. In addition, the expression levels of HDAC4 in PC3 tumors treated with YK-4-272 were decreased as shown in Fig. 4b. The immunohistochemical staining of HDAC4 and counterstaining with Hematoxylin were shown in Fig. 4c and d. These data show that YK-4-272 is a potential candidate for inhibiting human prostate tumor growth.

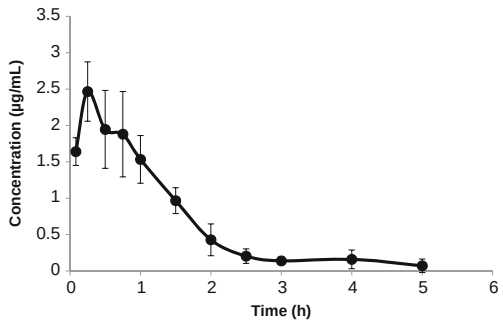


**Fig. 3** Plasma concentration of YK-4-272 after oral administration. 100 mg/kg YK-4-272 suspension was prepared with 0.5% Tween 80 aqueous solution and administered to rats (225 ± 10 g) by a gastric intubation. After an appropriate time interval, blood was collected and the concentration of YK-4-272 in the plasma was determined by HPLC. Each bar represents the mean ± S.D. ($n$=5).

## DISCUSSION

Previously, we demonstrated that the novel YK-4-272 localized in the cytoplasm, increased nuclear acetylation, and inhibited tubulin deacetylation in the cytoplasm of human prostate cancer cells (11). This observation suggested a new paradigm for understanding how HDAC inhibitors affect nuclear function of HDACs and furthered our discovery. Here, we have monitored and evaluated aqueous solubility, cell permeability, cytochrome P450 activity, *in vivo* pharmacokinetics and anti-tumor efficacy of the novel fluorescent class II HDAC selective inhibitor, YK-4-272, to predict oral bioavailability. YK-4-272 exhibits general properties required for oral bioavailability, and is effective as an anticancer agent as shown by inhibiting growth of human PC-3 tumor xenografts.

The FDA guidance on the biopharmaceutical classification system (BCS) shows four classifications of compounds based on their aqueous solubility and intestinal permeability for predicting the bioavailability of drugs (27,32). The four categories include high solubility-high

**Table IV** Pharmacokinetic Properties of YK-4-272 in Plasma After Oral Administration to SD Rats

| Parameter | YK-4-272 |
|---|---|
| $C_{max}$ (ng/mL) | 2467 |
| $T_{max}$ (h) | 0.25 |
| $T_{1/2}$ (h) | 0.87 |
| $AUC_{0\text{-last}}$ (ng × h/mL) | 3304 |
| MRT (h) | 1.3 |

AUC area under the curve; MRT mean residence time

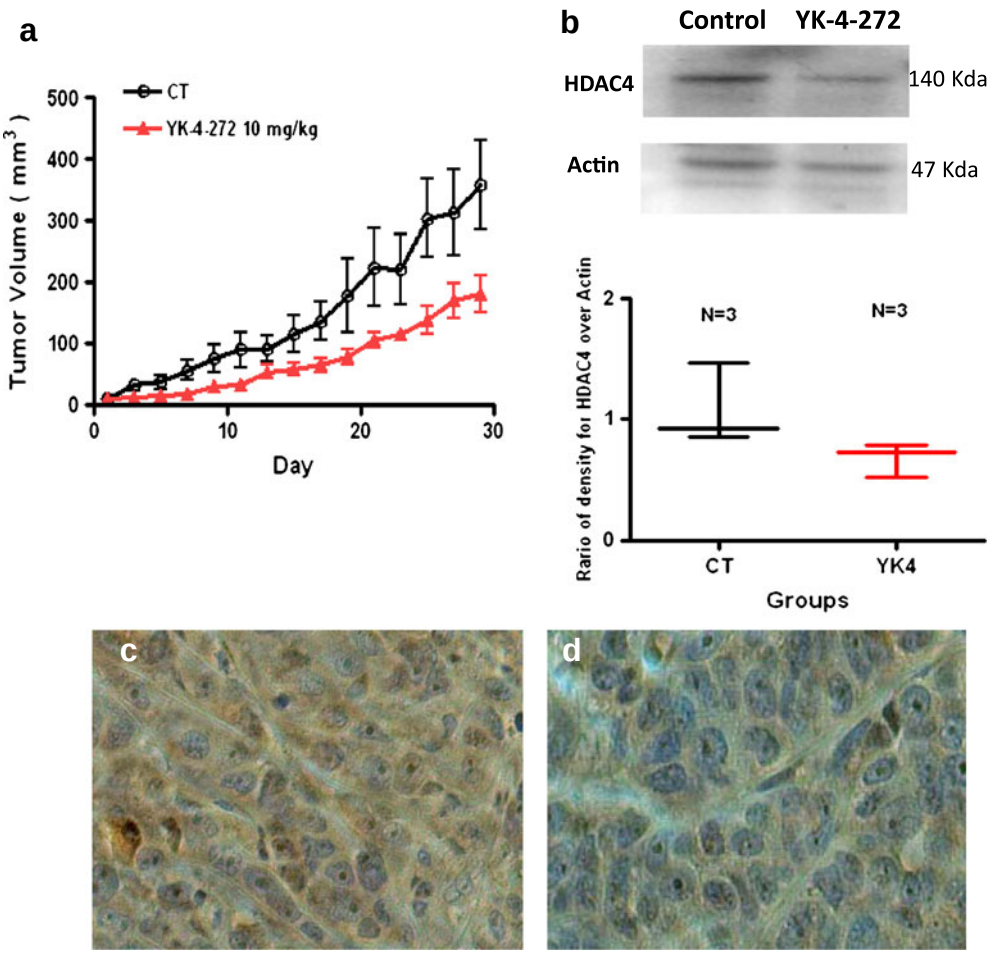


**Fig. 4** Antitumor activity of YK-4-272 on the growth of human prostate PC-3 tumor xenografts. Male athymic Balb/c nude mice were injected with PC-3 cells and the resulting tumors allowed growing for a week before i.p. injection once a day every other day with 10 mg/kg of YK-4-272 or vehicle in 1:1 PEG/PBS solution. (**a**) The tumor volumes were monitored up to 30 day. The tumor size of each mouse was measured by caliper and calculated by the formula: Length × width × height/2. Each bar represents the mean ± SEM ($n$=4). (**b**) Expression of HDAC4 in PC-3 tumor either 1) control (untreated) or 2) YK-4-272 treated. HDAC4 protein levels in tumor were analyzed by Western blotting. Actin expression is shown as a loading control. Each data point represents the mean value of optical density for HDAC4 from three experiments with similar results. (**c, d**) Tumors were stained with HDAC4 antibody and counterstained with Hematoxylin. (**c**) control (**d**) treated with YK-4-272.

permeability compounds (class I), low solubility-high permeability compounds (class II), high solubility-low permeability compounds (class III), and low solubility-low permeability compounds (class IV). Specifically for class I compounds, immediate release (IR) from solid oral-dosage formulation and rapid *in vitro* dissolution are required. To satisfy these conditions, a drug must be stable in the gastrointestinal tract, excipients used in the formulations must have no significant effect on the rate and extent of oral drug absorption, the drug should not have a narrow therapeutic index, and the product of the drug should be designed not to be absorbed in the oral cavity (33).

Pharmacokinetics and toxicology track potential drug actions and underlying mechanisms *in vivo*. Delivery of orally administered drugs requires efficient solubility, lipophilicity, stability, and permeability. The unitless octanol/water partition coefficient ($PC_{oct}$) is a predictor of drug absorption, or the capacity of a drug to partition into the lipophilic phase, represented by octanol (34). Generally, drugs with log $P$ values close to 2 are predicted to be absorbed completely into the blood system. A log $P$ value over 4 results in decreased permeability because of low aqueous solubility and slower partition (34,35). Furthermore, the absorption of drugs having more than 90% of the orally administered dose has high permeability (33,36). YK-4-272's solubility shows that it is efficient for oral formulation, and higher than is reported for SAHA, an FDA approved HDAC inhibitor and soluble in DMSO (37). YK-4-272's chemical stability and apparent partition coefficient predict YK-4-272 as stable and absorbable completely in the gastrointestinal tract.

The transport of drugs across the intestinal epithelium has at least four different routes. These include passive transcellular and paracellular, carrier mediated, and

transcytosis routes (34). Caco-2 cell monolayers have been used to study drug transport, elicited the drug transport by different pathways across the intestinal epithelium even though the best correlation with the absorption *in vivo* is from passively transported drugs (34). YK-4-272 exhibits high permeability and this is comparable to the well-known high permeability marker, propranolol, without involvement of P-gp and MRP. Therefore, YK-4-272 is predicted to be absorbed completely as a highly permeable compound in the gastrointestinal tract.

Compounds that have high rates of metabolism by several enzymes may exhibit low bioavailability because of phase I cytochrome P450 oxidations or phase II conjugations in the liver (26). Human liver microsomes provide an appropriate *in vitro* metabolic model and contain CYP450 enzymes and some phase II conjugating enzymes (26). In pooled HLM, only 14% of YK-4-272 is metabolized over 2 h and in the presence of cDNA-expressed human CYP proteins, YK-4-272 exhibited inductive effect on CYP2C9 and CYP3A4 enzymes and did not inhibit the evaluated CYP panel. These *in vitro* studies suggest that CYP2C9 and CYP3A4 may be key oxidative pathways for metabolic clearance of YK-4-272. Enzymatic stability experiments with YK-4-272 on the basis of hepatic intrinsic clearance may be needed to predict this compound's metabolism more accurately (38,39).

Oral pharmacokinetic evaluation of YK-4-272 resulted in a generally favorable metabolic profile as judged from the $C_{max}$ and AUC. Furthermore, 10 mg/kg dose of YK-4-272 effectively reduces tumor growth in mice by about 50% as compared to control mice over 30 days of treatment. HDAC4 protein levels in tumor were also decreased by YK-4-272 treatment. Based on these data, YK-4-272 offers good predicted oral bioavailability and metabolism at doses required for tumor regression in a model system.

## CONCLUSION

In conclusion, our findings provide initial preclinical pharmacologic data for the HDAC shuttling disruptor, YK-4-272 in support of good bioavailability following oral administration. YK-4-272 is predicted to be absorbed completely in the gastrointestinal tract with low toxicity. This study provides support for further preclinical studies to elucidate the absorption, distribution, metabolism, and excretion properties of YK-4-272 as an anticancer drug.

## ACKNOWLEDGMENTS AND DISCLOSURES

We thank Youngmi Kim, Yunjin Jung, and Mikell Paige for helpful discussions and technical assistance. This study was supported by National Institutes of Health grants (NIH/NCI P30 CA51008).

## REFERENCES

1. Laherty CD, Yang WM, Sun JM, Davie JR, Seto E, Eisenman RN. Histone deacetylases associated with the mSin3 corepressor mediate mad transcriptional repression. Cell. 1997;89:349–56.
2. Imai S, Armstrong CM, Kaeberlein M, Guarente L. Transcriptional silencing and longevity protein Sir2 is an NAD-dependent histone deacetylase. Nature. 2000;403:795–800.
3. de Ruijter AJ, van Gennip AH, Caron HN, Kemp S, van Kuilenburg AB. Histone deacetylases (HDACs): characterization of the classical HDAC family. Biochem J. 2003;370:737–49.
4. Finnin MS, Donigian JR, Pavletich NP. Structure of the histone deacetylase SIRT2. Nat Struct Biol. 2001;8:621–5.
5. Gallinari P, Di Marco S, Jones P, Pallaoro M, Steinkuhler C. HDACs, histone deacetylation and gene transcription: from molecular biology to cancer therapeutics. Cell Res. 2007;17:195–211.
6. Ashburner BP, Westerheide SD, Baldwin Jr AS. The p65 (RelA) subunit of NF-kappaB interacts with the histone deacetylase (HDAC) corepressors HDAC1 and HDAC2 to negatively regulate gene expression. Mol Cell Biol. 2001;21:7065–77.
7. Blagosklonny MV, Robey R, Sackett DL, Du L, Traganos F, Darzynkiewicz Z, *et al.* Histone deacetylase inhibitors all induce p21 but differentially cause tubulin acetylation, mitotic arrest, and cytotoxicity. Mol Cancer Ther. 2002;1:937–41.
8. Naryzhny SN, Lee H. The post-translational modifications of proliferating cell nuclear antigen: acetylation, not phosphorylation, plays an important role in the regulation of its function. J Biol Chem. 2004;279:20194–9.
9. Varshochi R, Halim F, Sunters A, Alao JP, Madureira PA, Hart SM, *et al.* ICI182,780 induces p21Waf1 gene transcription through releasing histone deacetylase 1 and estrogen receptor alpha from Sp1 sites to induce cell cycle arrest in MCF-7 breast cancer cell line. J Biol Chem. 2005;280:3185–96.
10. Halkidou K, Cook S, Leung HY, Neal DE, Robson CN. Nuclear accumulation of histone deacetylase 4 (HDAC4) coincides with the loss of androgen sensitivity in hormone refractory cancer of the prostate. Eur Urol. 2004;45:382–9.
11. Kong Y, Jung M, Wang K, Grindrod S, Velena A, Lee S, *et al.* Histone deacetylase cytoplasmic trapping by a novel fluorescent HDAC inhibitor. Mol Cancer Ther 2011;10:1591–99.
12. Doh MJ, Jung YJ, Kim I, Kong HS, Kim YM. Synthesis and *in vitro* properties of prednisolone 21-sulfate sodium as a colon-specific prodrug of prednisolone. Arch Pharm Res. 2003;26:258–63.
13. Lee J, Rho J, Yang Y, Kong H, Jung Y, Kim Y. Synthesis and *in vitro* evaluation of N-nicotinoylglycyl-2-(5-fluorouracil-1-yl)-D, L-glycine as a colon-specific prodrug of 5-fluorouracil. J Drug Target. 2007;15:199–205.
14. Uchida M, Fukazawa T, Yamazaki Y, Hashimoto H, Miyamoto Y. A modified fast (4 day) 96-well plate Caco-2 permeability assay. J Pharmacol Toxicol Methods. 2009;59:39–43.
15. Frederick KS, Maurer TS, Kalgutkar AS, Royer LJ, Francone OL, Winter SM, *et al.* Pharmacokinetics, disposition and lipid-modulating activity of 5-{2-[4-(3,4-difluorophenoxy)-phenyl]-ethylsulfamoyl}-2-methyl-benzoic acid, a potent and subtype-selective peroxisome proliferator-activated receptor alpha agonist in preclinical species and human. Xenobiotica. 2009;39:766–81.
16. Bey E, Marchais-Oberwinkler S, Werth R, Negri M, Al-Soud YA, Kruchten P, *et al.* Design, synthesis, biological evaluation and pharmacokinetics of bis(hydroxyphenyl) substituted azoles, thiophenes, benzenes, and aza-benzenes as potent and selective non-steroidal inhibitors of 17beta-hydroxysteroid dehydrogenase type 1 (17beta-HSD1). J Med Chem. 2008;51:6725–39.
17. Madgula VL, Avula B, Pawar RS, Shukla YJ, Khan IA, Walker LA, *et al. in vitro* metabolic stability and intestinal transport of

P57AS3 (P57) from Hoodia gordonii and its interaction with drug metabolizing enzymes. Planta Med. 2008;74:1269–75.
18. Obach RS, Baxter JG, Liston TE, Silber BM, Jones BC, MacIntyre F, *et al.* The prediction of human pharmacokinetic parameters from preclinical and *in vitro* metabolism data. J Pharmacol Exp Ther. 1997;283:46–58.
19. OECD. Acute oral toxicity-up and down procedure. OECD Guides for testing of chemicals. 2001.
20. Sheikh KD, Banerjee PP, Jagadeesh S, Grindrod SC, Zhang L, Paige M, *et al.* Fluorescent epigenetic small molecule induces expression of the tumor suppressor ras-association domain family 1A and inhibits human prostate xenograft. J Med Chem. 2010;53: 2376–82.
21. Jeanne E. Phillips AA. MultiScreen® Caco-2 Assay System Protocol Note. Optimization of Caco-2 cell growth and differentiation for drug transport assay studies using a 96-well assay system. Millipore Corporation 2003:1–12.
22. Artursson P, Karlsson J. Correlation between oral drug absorption in humans and apparent drug permeability coefficients in human intestinal epithelial (Caco-2) cells. Biochem Biophys Res Commun. 1991;175:880–5.
23. GENTEST/BDBiosciencesCompany. CYP2C9/MFC high throughput inhibitor screening kit instruction manual. 2002.
24. Sambuy Y, De Angelis I, Ranaldi G, Scarino ML, Stammati A, Zucco F. The Caco-2 cell line as a model of the intestinal barrier: influence of cell and culture-related factors on Caco-2 cell functional characteristics. Cell Biol Toxicol. 2005;21:1–26.
25. Konsoula Z, Jung M. Involvement of P-glycoprotein and multidrug resistance associated protein 1 on the transepithelial transport of a mercaptoacetamide-based histone-deacetylase inhibitor in Caco-2 cells. Biol Pharm Bull. 2009;32:74–8.
26. Kerns EH, Di L. Pharmaceutical profiling in drug discovery. Drug Discov Today. 2003;8:316–23.
27. FDA/CDER. Guidance for industry. Waiver of *in vivo* bioavailability and bioequivalence studies for immediate-release solid oral dosage forms based on a biopharmaceutics classification system. http://www.fda.gov/cder/guidance/index.htm 2000:1–13.
28. Royer I, Monsarrat B, Sonnier M, Wright M, Cresteil T. Metabolism of docetaxel by human cytochromes P450: interactions with paclitaxel and other antineoplastic drugs. Cancer Res. 1996;56:58–65.
29. Long L, Dolan ME. Role of cytochrome P450 isoenzymes in metabolism of O(6)-benzylguanine: implications for dacarbazine activation. Clin Cancer Res. 2001;7:4239–44.
30. Crespi CL, Miller VP, Penman BW. Microtiter plate assays for inhibition of human, drug-metabolizing cytochromes P450. Anal Biochem. 1997;248:188–90.
31. Clayton AL, Hazzalin CA, Mahadevan LC. Enhanced histone acetylation and transcription: a dynamic perspective. Mol Cell. 2006;23:289–96.
32. Amidon GL, Lennernas H, Shah VP, Crison JR. A theoretical basis for a biopharmaceutic drug classification: the correlation of *in vitro* drug product dissolution and *in vivo* bioavailability. Pharm Res. 1995;12:413–20.
33. Yazdanian M, Briggs K, Jankovsky C, Hawi A. The "high solubility" definition of the current FDA Guidance on Biopharmaceutical Classification System may be too strict for acidic drugs. Pharm Res. 2004;21:293–9.
34. Artursson P, Palm K, Luthman K. Caco-2 monolayers in experimental and theoretical predictions of drug transport. Adv Drug Deliv Rev. 2001;46:27–43.
35. Wils P, Warnery A, Phung-Ba V, Legrain S, Scherman D. High lipophilicity decreases drug transport across intestinal epithelial cells. J Pharmacol Exp Ther. 1994;269:654–8.
36. FDA/CDER. Guidance for industry. Bioavailability and Bioequivalence Studies for Orally Administered Drug Products-General Considerations. http://www.fda.gov/cder/guidance/index.htm 2003:1–23.
37. Novotny-Diermayr V, Sangthongpitag K, Hu CY, Wu X, Sausgruber N, Yeo P, *et al.* SB939, a novel potent and orally active histone deacetylase inhibitor with high tumor exposure and efficacy in mouse models of colorectal cancer. Mol Cancer Ther. 2010;9:642–52.
38. Obach RS, Walsky RL, Venkatakrishnan K. Mechanism-based inactivation of human cytochrome p450 enzymes and the prediction of drug-drug interactions. Drug Metab Dispos. 2007;35:246–55.
39. Obach RS, Walsky RL, Venkatakrishnan K, Houston JB, Tremaine LM. *in vitro* cytochrome P450 inhibition data and the prediction of drug-drug interactions: qualitative relationships, quantitative predictions, and the rank-order approach. Clin Pharmacol Ther. 2005;78:582–92.